Tenth U.S. National Conference on Earthquake Engineering
Frontiers of Earthquake Engineering
July 21-25, 2014
Anchorage, Alaska

EFFECT OF INTENSITY BOUNDS ON THE SEISMIC SAFETY OF STRUCTURES

N. Lazar[1] and M. Dolšek[2]

ABSTRACT

The seismic safety of structures is often communicated with the mean annual frequency of collapse, which can be obtained by integrating the collapse fragility function with the seismic hazard over the entire range of ground motion intensity (i.e. from zero to infinity). It is argued that this approach is unphysical and may lead to overestimation of collapse risk. In order to study whether the mean annual frequency of collapse is overestimated if the intensity bounds are not considered in a physically consistent manner, a closed-form solution for assessing the proportion of the mean annual frequency of limit-state exceedance as a function of integration limits was introduced and discussed. It was shown that the impact of integration limits depends on the median collapse intensity, the corresponding dispersion and the slope of the hazard curve in the log domain. The approach to estimate the impact of the intensity bounds on collapse risk was applied to six reinforced concrete frame structures located in Ljubljana, a moderate seismic region, or in Paris, a low seismic region. It is shown that the mean annual frequency of collapse can be highly overestimated if intensity bounds are not considered in the risk assessment procedure. More significant impact of the lower integration limit can be expected if the collapse risk assessment is based on the peak ground acceleration, whereas the opposite is true when assessment is based on spectral acceleration at the fundamental vibration period.

[1]PhD Student, Faculty of Civil and Geodetic Engineering, University of Ljubljana, Ljubljana, Slovenia
[2]Asocciate Professor, Faculty of Civil and Geodetic Engineering, University of Ljubljana, Ljubljana, Slovenia

Lazar N, Dolšek M. Effect of intensity bounds on the seismic safety of structures. *Proceedings of the 10th National Conference in Earthquake Engineering*, Earthquake Engineering Research Institute, Anchorage, AK, 2014.

Effect of Intensity Bounds on the Seismic Safety of Structures

N. Lazar[1] and M. Dolšek[2]

ABSTRACT

The seismic safety of structures is often communicated with the mean annual frequency of collapse, which can be obtained by integrating the collapse fragility function with the seismic hazard over the entire range of ground motion intensity (i.e. from zero to infinity). It is argued that this approach is unphysical and may lead to overestimation of collapse risk. In order to study whether the mean annual frequency of collapse is overestimated if the intensity bounds are not considered in a physically consistent manner, a closed-form solution for assessing the proportion of the mean annual frequency of limit-state exceedance as a function of integration limits was introduced and discussed. It was shown that the impact of integration limits depends on the median collapse intensity, the corresponding dispersion and the slope of the hazard curve in the log domain. The approach to estimate the impact of the intensity bounds on collapse risk was applied to six reinforced concrete frame structures located in Ljubljana, a moderate seismic region, or in Paris, a low seismic region. It is shown that the mean annual frequency of collapse can be highly overestimated if intensity bounds are not considered in the risk assessment procedure. More significant impact of the lower integration limit can be expected if the collapse risk assessment is based on the peak ground acceleration, whereas the opposite is true when assessment is based on spectral acceleration at the fundamental vibration period.

Introduction

Many procedures for the assessment of seismic risk have been developed and used for the purpose of research and for the calibration of building codes. Seismic risk is often communicated by the mean annual frequency (MAF) of limit state exceedance, which is obtained by integrating the collapse fragility function with the seismic hazard over the entire range of ground motion intensity (e.g. [1-5]). However, building codes for earthquake resistant design provide a certain level of strength and ductility of buildings. Therefore from the engineering-focused viewpoint one might argue that there is no such ground motion which would cause collapse given intensity, which is below a certain threshold value. On the contrary, the upper bound ground-motion intensity also exists at a specific site, and is associated with the physics of earthquakes, tectonic regime at the site of the building under investigation and the geology of terrain [6,7]. By integrating the risk equation over the entire range of intensity, even the lower intensities, which cannot cause the occurrence of a limit state (e.g. collapse) and larger intensities, which are not possible at an observed location, are taken into account. In general, such approach causes an overestimation of seismic risk. This issue was recently addressed elsewhere [8]. Herein simple formulas to estimate the impact of integration limits on seismic risk and their threshold values

[1]PhD Student, Faculty of Civil and Geodetic Engineering, University of Ljubljana, Ljubljana, Slovenia
[2]Asocciate Professor, Faculty of Civil and Geodetic Engineering, University of Ljubljana, Ljubljana, Slovenia

Lazar N, Dolšek M. Effect of intensity bounds on the seismic safety of structures. *Proceedings of the 10th National Conference in Earthquake Engineering*, Earthquake Engineering Research Institute, Anchorage, AK, 2014.

are summarized and discussed. The approach to estimate the impact of the intensity bounds on collapse risk was applied to six concrete frame structures located in Ljubljana, a moderate seismic region, or in Paris, a low seismic region. An emphasis is given on evaluating the impact of the intensity bounds for two different intensity measures, the peak ground acceleration and the spectral acceleration at the first vibration period.

Seismic Risk Assessment with Consideration of Intensity Bounds

Seismic risk expressed with the mean annual frequency (MAF) of limit-state exceedance can be determined by integrating the limit-state fragility function $P(LS|IM = im)$ of the structure over the seismic hazard curve $H(im)$ (e.g. [1, 3, 4, 9]):

$$\lambda_{LS} = \int_0^{\infty} P\left(LS \middle| IM = im\right) \cdot \left| \frac{dH\left(im\right)}{d\left(im\right)} \right| \cdot d\left(im\right). \tag{1}$$

An approximate closed-form solution of Eq. 1 was obtained by assuming a linear seismic hazard in log-log coordinates and a log-normal distribution of limit-state intensity im_{LS} (e.g. [5, 9, 10]):

$$\lambda_{LS} = H\left(im_{LS,50}\right) \cdot \exp\left(\frac{1}{2} \cdot k^2 \cdot \beta_{im,LS}^2\right) \tag{2}$$

where $im_{LS,50}$ and $\beta_{im,LS}$ are the median limit-state intensity and the corresponding standard deviation of natural logarithms and k is the slope of the hazard function in log-log coordinates. Eq. 2 was obtained by integrating Eq. 1 for the entire range of intensities. Recently the impact of the lower and the upper integration limit on MAF of limit-state exceedance was investigated by defining the following two ratios [8]:

$$\Delta\lambda_{LS,im1} = \frac{\overline{\lambda}_{LS,im1}}{\lambda_{LS}}, \Delta\lambda_{LS,im2} = \frac{\overline{\lambda}_{LS,im2}}{\lambda_{LS}} \tag{3}$$

where

$$\overline{\lambda}_{LS,im1} = \int_{im_1}^{\infty} P\left(LS \middle| IM = im\right) \cdot \left| \frac{dH\left(im\right)}{d\left(im\right)} \right| \cdot d\left(im\right) \tag{4}$$

$$\overline{\lambda}_{LS,im2} = \int_0^{im_2} P\left(LS \middle| IM = im\right) \cdot \left| \frac{dH\left(im\right)}{d\left(im\right)} \right| \cdot d\left(im\right) \tag{5}$$

In order to understand which parameters have the greatest impact on the MAF of limit-state exceedance, it was helpful to solve the Eqs. 4 and 5 in close-form [8]:

$$\bar{\lambda}_{LS,im1} = \lambda_{LS} \cdot \frac{1}{2}\left(1 - \text{erf}\left[\frac{1}{\sqrt{2}\beta_{im,LS}}\left(k\beta_{im,LS}^2 + \ln\left(\Delta im_1\right)\right)\right]\right) \tag{6}$$

$$\bar{\lambda}_{LS,im2} = \lambda_{LS} \cdot \frac{1}{2}\left(1 + \text{erf}\left[\frac{1}{\sqrt{2}\beta_{im,LS}}\left(k\beta_{im,LS}^2 + \ln\left(\Delta im_2\right)\right)\right]\right) \tag{7}$$

where Δim_1 and Δim_2 represent, respectively, the ratio between the lower integration limit and the median limit-state intensity, and the ratio between the upper integration limit and the median limit-state intensity:

$$\Delta im_1 = \frac{im_1}{im_{LS,50}},\ \Delta im_2 = \frac{im_2}{im_{LS,50}} \tag{8}$$

and erf[x] is the error function, which takes a value between -1 and 1 and is defined as follows:

$$\text{erf}\left[x\right] = \frac{2}{\sqrt{\pi}}\int_0^x \exp\left[-\tau^2\right] d\tau \tag{9}$$

Based on Eqs. 6 and 7 and an assumption that the 3% error for assessing the MAF of limit-state exeedance is negligible, it was shown [8] that the limits of integration may become important if at least one of the two conditions is met:

$$im_{1,T} = im_{LS,50} \cdot \exp\left[-2\beta_{im,LS} - k\beta_{im,LS}^2\right], \tag{10}$$

$$im_{2,T} = im_{LS,50} \cdot \exp\left[2\beta_{im,LS} - k\beta_{im,LS}^2\right]. \tag{11}$$

It can be concluded that the lower integration limit im_1 becomes important if its value, which varies from structure to structure, is greater than its threshold value $im_{1,T}$ (Eq. 10). The logic is different in the case of the upper integration limit im_2 since the impact of im_2 on the assessment of seismic risk becomes important if $im_2<im_{2,T}$ (Eq. 11). In this paper a quantitative measure for the impact of integration limits on the mean annual frequency of exceeding a designated limit state is analysed by the ratios $\Delta\lambda_{LS,im1}$ and $\Delta\lambda_{LS,im2}$ (Eqs. 3 to 5), which are depicted in Fig. 1 as a function of the logarithmic standard deviation $\beta_{im,LS}$ for three hazard slopes k and selected values of Δim_1 and Δim_2 (Eq. 8). It is evident that an increased impact on $\Delta\lambda_{LS,im1}$ is caused by increasing any of the parameters (Δim_1, $\beta_{im,LS}$, k) which affect $\Delta\lambda_{LS,im1}$. The opposite trend can be observed in the case of $\Delta\lambda_{LS,im2}$, since the impact on the MAF of limit-state exceedance is reduced by increasing any of the observed parameters (Δim_1, $\beta_{im,LS}$, k). For example, if $\beta_{im,LS}$ is less than 0.3 and k is less than 3, the lower integration limit does not have an impact on the MAF of limit state exceedance, even if its value is equal to 50% of the median limit-state capacity. Nevertheless, in the case when $\beta_{im,LS}$ > 0.3 the impact of the lower integration limit may have a significant effect, which is not negligible especially for large values of the parameter k. On the contrary, the impact of the upper integration limit on the MAF of limit-state exceedance is not so severe when Δim_2 > 1 and $\beta_{im,LS}$ > 0.3 and is not negligible in other cases.

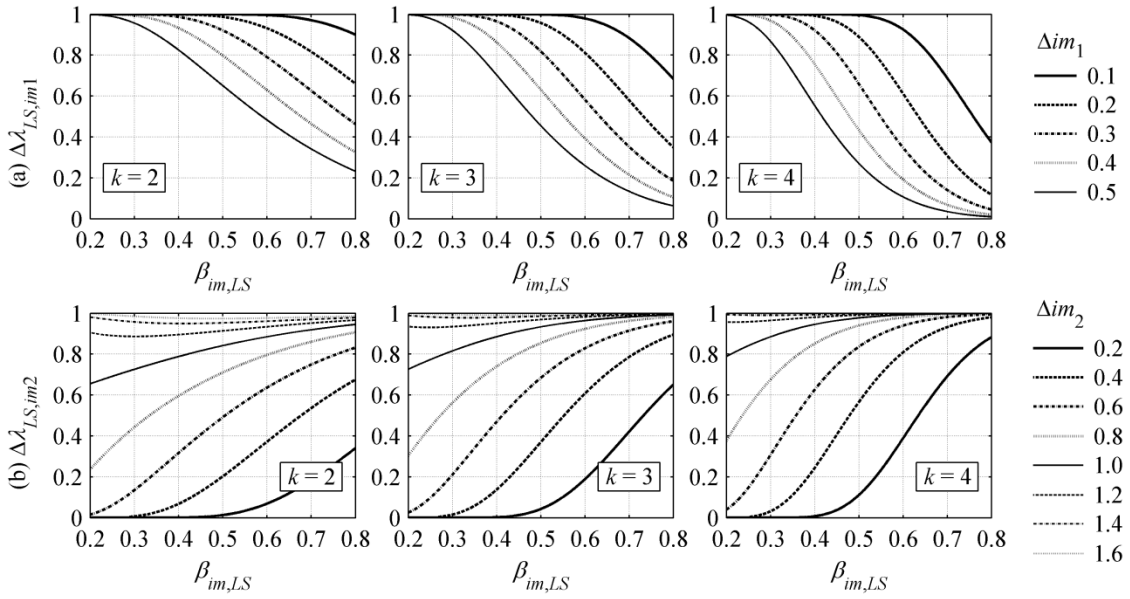

Figure 1. The (a) $\Delta\lambda_{LS,im1}$ and (b) $\Delta\lambda_{LS,im2}$ as a function of $\beta_{im,LS}$ presented for selected values of k and Δim_1 or Δim_2.

Impact of Intensity Bounds on the Collapse Risk of Code-Conforming RC Frames

The impact of integration limits on collapse risk was estimated for six reinforced concrete frame buildings depicted in Fig. 2 [8]. In this demonstrative example we examine how the consideration of different intensity measures (peak ground acceleration (a_g) and spectral acceleration $S_a(T_1)$) affect the MAF of collapse when intensity bounds are taken into account, since this phenomenon was not considered in the previous study [8].

All the buildings were designed according to Eurocode 8 provisions [11]. The reference a_g ($a_{g,R}$) on type A ground (rock), the soil type at the location of the building, the design a_g at the location of the building and the adopted ductility class are summarized in Table 1. The material class for concrete varied slightly from case to case (Table 1). The seismic hazard for Ljubljana, Slovenia, was obtained by using EZ-FRISK [12,13]. The corresponding hazard curve (k) was estimated by fitting a straight line to the hazard curve in log-log coordinates with the method of least squares. It amounted 2.9 in the case of a_g and between 2.10 and 2.24 for $S_a(T_1)$, depending on the fundamental period of the structure. For simplicity reasons a mean value of 2.2 was taken into account for the spectral acceleration at T_1. Additionally it was assumed that buildings were located in Paris, a low seismic region with high value of k = 4.8 [14]. The intensity measure considered in these examples was just a_g, since seismic hazard curves for $S_a(T_1)$ were not available. Only the effect of the high slope of the hazard curve (k) on the proportion of the MAF of collapse (Eq. 3), if the lower intensity bound was taken into account, is demonstrated. It should be noted that the values of Δim_1 and the standard deviation of the natural logarithms of the $a_{g,C}$ were assumed on the basis of structures designed for a moderate seismic region. This assumption was made since only relative values of collapse intensities were required to calculate the proportion of the MAF of collapse, which most probably do not significantly depend on the design peak ground acceleration.

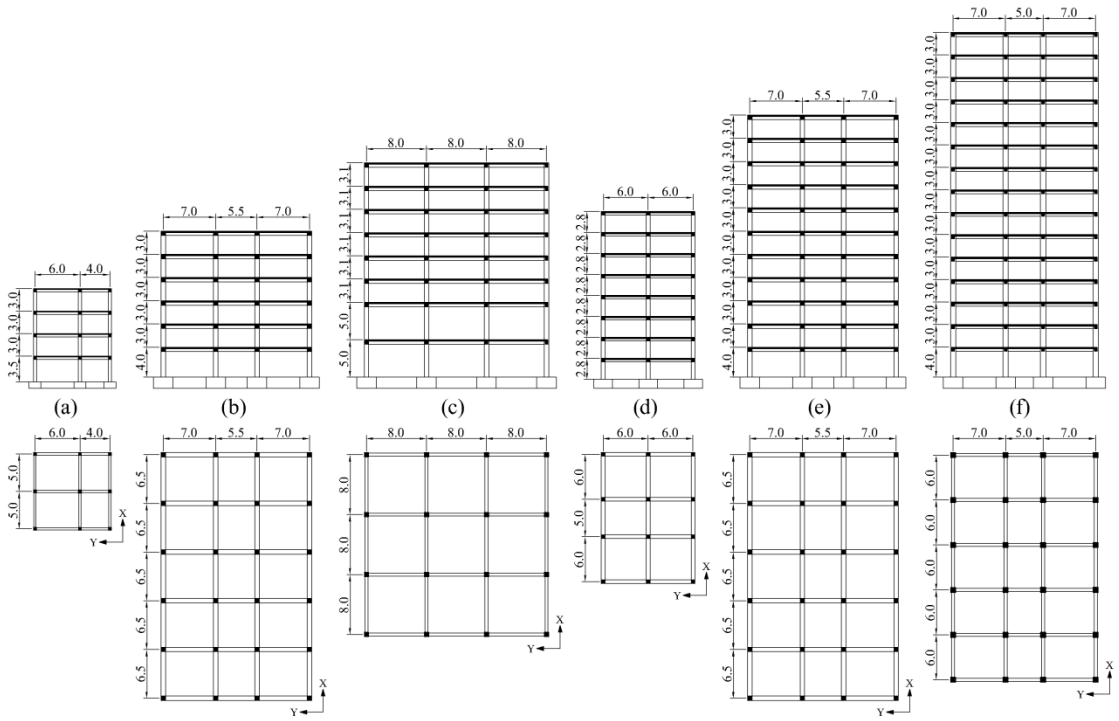

Figure 2. Elevation and plan views of the analysed buildings: (a) 4-storey, (b) 6-storey, (c) 8-storey irregular in elevation, (d) 8-storey regular, (e) 11-storey and (f) 15-storey.

Table 1. The first vibration period T_1, the design peak ground acceleration at rock outcrop $a_{g,R}$, the soil type, the design peak ground acceleration at the building's site, the ductility class and the material class for the six investigated buildings.

Model	T_1 (s)	$a_{g,R}$ (g)	Soil type	a_g (g)	Ductility class	Concrete class	Steel class
4-storey	0.80	0.25	B	0.3	DCH	C25/30	S500
6-storey	1.00	0.25	B	0.3	DCM	C35/45	S500
8-storey irregular	1.76	0.20	B	0.24	DCM	C30/37	S500
8-storey regular	1.29	0.25	C	0.29	DCM	C30/37	S500
11-storey	1.57	0.25	B	0.3	DCM	C35/45	S500
15-storey	1.96	0.25	B	0.3	DCM	C25/30 ÷ C40/50	S500

Incremental dynamic analysis was used to determine the collapse capacity im_C. The structural models of the six buildings were consistent with Eurocode 8 requirements for the modeling of structures. All the analyses were performed with OpenSees [15] using the PBEE toolbox [16]. Each building was exposed to sixty ground-motions, which were selected based on the algorithm proposed by Jayaram et al. [17] in order to match a target spectrum. A sample of sixty values of im_C was obtained to which a log-normal distribution was fitted in order to estimate the median collapse intensity $im_{C,50}$ and the corresponding logarithmic standard deviation $\beta_{im,C}$. The minimum intensity causing collapse was assumed as the lower integration limit im_1 of the risk equation. The results are given in Table 2, where threshold values for the lower and upper integration limit determined with Eqs. 10 and 11 are also presented.

The estimated minimum collapse intensity was quite high (Table 2) since all the buildings were designed according to current design standards [11]. For example, the largest im_1 was observed in the case of the 4-storey building, which is the only building in the study that was designed for ductility class high (DCH), so that more rigorous capacity design criteria were applied. The smallest value of im_1 was observed for the irregular 8-storey building. The height of the first and the second floor of this building was about 60% greater than the height of other storeys and consequently some ground motions caused collapse at low levels of intensity due to a soft-storey mechanism of collapse. The standard deviation of the logarithms of the collapse intensity based on $S_a(T_1)$ ($\beta_{Sa,C} \in [0.35, 0.44]$) was smaller than that based on a_g ($\beta_{ag,C} \in [0.53, 0.71]$). Consequently, the impact of im_1 on the MAF of collapse was, in general, smaller and the impact of im_2 was greater in the case of spectral acceleration $S_a(T_1)$ (see Fig. 1). The minimum collapse intensities $a_{g,1}$ and $S_{a,1}$ were, in most cases, higher than the corresponding threshold values. Seismic risk was therefore overestimated if the lower integration limit was not taken into account with the exception of some cases, i.e. the 15-storey building in the case of a_g and for the 8-storey irregular and 11-storey building when $S_a(T_1)$ was used as an intensity measure for the assessment of collapse risk. The ratio of the threshold value and the median collapse intensity $\Delta im_{1,T}$ ranges from 0.06 to 0.15 when based on a_g and from 0.27 to 0.38 when based on $S_a(T_1)$, where higher values for $S_a(T_1)$ indicate a possibly lower impact of the lower integration limit.

Table 2. The median collapse intensity $im_{C,50}$ and the corresponding standard deviation of log data $\beta_{im,C}$, the minimum collapse intensity im_1 and threshold values $im_{1,T}$ and $im_{2,T}$. Results are presented for two intensity measures, peak ground acceleration a_g and spectral acceleration S_a at the first vibration period.

Model	$a_{g,C,50}$ (g)	$\beta_{ag,C}$	$a_{g,1}$ (g)	$a_{g,1,T}$ (g)	$a_{g,2,T}$ (g)	$S_{a,C,50}$ (g)	$\beta_{Sa,C}$	$S_{a,1}$ (g)	$S_{a,1,T}$ (g)	$S_{a,2,T}$ (g)
4-storey	1.91	0.58	0.68	0.23	2.30	2.53	0.39	1.03	0.83	3.95
6-storey	1.81	0.66	0.56	0.14	1.92	1.91	0.42	0.80	0.56	3.00
8-storey irregular	1.45	0.71	0.24	0.08	1.39	0.92	0.44	0.23	0.25	1.45
8-storey regular	1.34	0.53	0.31	0.21	1.71	1.37	0.36	0.65	0.50	2.12
11-storey	2.25	0.59	0.45	0.25	2.67	1.57	0.37	0.50	0.55	2.43
15-storey	2.32	0.54	0.33	0.34	2.93	1.28	0.35	0.54	0.49	1.97

The estimates of $\Delta\lambda_{C,im1}$ (Eqs. 3 and 4) are presented in Fig. 4 for all six buildings in analogy to Fig. 1. In this case the slope of the hazard curve is considered also for the location of Paris if $\Delta\lambda_{C,im1}$ is assessed on the basis of peak ground acceleration. It can be seen that for the region of Ljubljana ($k = 2.9$) the minimum value of $\Delta\lambda_{C,ag1}$ was around 0.45 (Fig. 4(a)) for the 6-storey structure. However, if the structure would be located in Paris, the value of $\Delta\lambda_{C,ag1}$ would be reduced below 0.1 (Fig. 4(b)), indicating that Eq. 2 would provide (roughly speaking) a tenfold overestimation of collapse risk just by neglecting the impact of the lower integration limit. The estimated values of $\Delta\lambda_{C,Sa1}$, which were obtained just for the case when buildings were located in Ljubljana, were greater than $\Delta\lambda_{C,ag1}$. This indicates that the effect of the lower integration limit on the collapse risk was smaller if the assessment was based on $S_a(T_1)$. Such an impact was the consequence of reduced values of $\beta_{Sa,C}$ and k in the case if assessment was based on the $S_a(T_1)$ rather than the a_g.

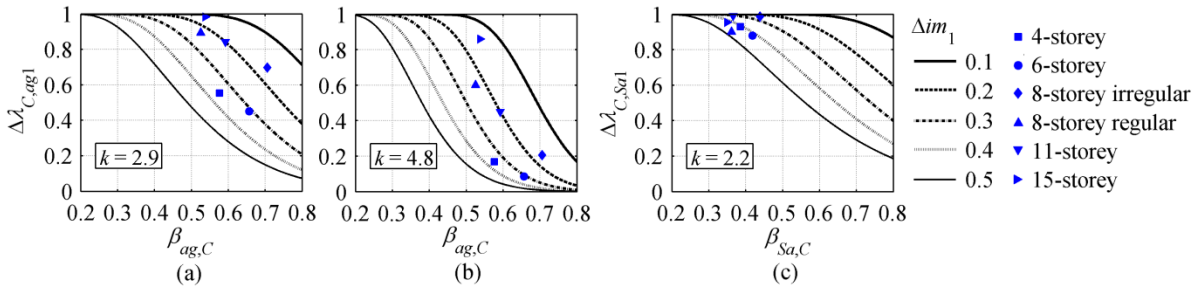

Figure 4. Estimates of $\Delta\lambda_{C,im1}$ corresponding to the collapse cases of the analysed buildings for (a) a_g and k = 2.9, (b) a_g and k = 4.8 and (c) $S_a(T_1)$ and k = 2.2.

The upper bounds of a_g and $S_a(T_1)$ were estimated by using ground motion prediction equations (GMPEs) proposed by Sabetta and Pugliese [18], Akkar and Bommer [19] and Bindi et al. [20]. Although the model proposed by Sabetta and Pugliese is outdated, it was taken into account since it was used for the hazard analysis of Slovenia [21]. For comparison reasons, the upper intensity bounds (im_2) were estimated by assuming an upper magnitude 6.5 or 7.0, which is consistent with the hazard analysis for Slovenia [21], two different values for the standard deviation above the logarithmic mean (2σ and 3σ), which is consistent with the sensitivity study for the seismic hazard at the Krško NPP [22], and a source-to-site distance R_{jb} of 0 km and 5 km. A strike-slip faulting style was assumed according to Lapajne et al. [21] and, for simplicity reasons, site class B according to Eurocode 8 [11] was assumed for all buildings. The estimated upper intensity limits with median values and standard deviations are presented in Tables 3 and 4. The results for spectral acceleration are presented only for the 4-storey building (Table 4) due to simplicity reasons. It should be noted that the median and the upper bound intensities associated with different GMPEs were not completely compatible since they were based on different definitions of the horizontal component of motion. Sabetta and Pugliese considered the maximum horizontal component, whereas Akkar and Bommer and Bindi et al. estimate the geometric mean of horizontal components. In general, the horizontal component of motion predicted according to different GMPEs should be adjusted to the horizontal component used in response history analysis. A procedure for such adjustments was proposed by Beyer and Bommer [23], however, this effect was herein neglected, since consideration of compatibility between the horizontal-component definitions used in GMPEs and the risk equation had insignificant impact on the $\Delta\lambda_{C,im2}$.

From Tables 3 and 4 it can be observed how the GMPE, the truncation level and the upper magnitude affected im_2 and consequently the estimated seismic risk. The lowest values of im_2 were mostly obtained with the GMPE proposed by Sabetta and Pugliese or Akkar and Bommer, while the largest values of im_2 were obtained with the GMPE proposed by Bindi et al. As expected the predicted im_2 increased with the truncation level and magnitude and decreased with source-to-site distance. The lowest estimated value of the upper integration limit $a_{g,2}$=1.14 g is quite lower than the threshold value $a_{g,2,T}$ (Table 2) for all structures located in Ljubljana, which can potentially indicate a large impact on the MAF of collapse. On the other hand, the largest value of $a_{g,2}$=4.66 g was higher than its threshold value and no impact on the MAF of collapse was expected. The largest predicted value of $S_{a,2}$ for the 4-storey structure amounted to 10.51 g (Table 4) and was higher than $S_{a,2,T}$ = 3.95 g (Table 2) therefore it would not affect seismic risk. However, the lowest predicted value amounted to 1.58 g, which was quite smaller

than the corresponding threshold value, indicating a potentially large impact on the collapse risk assessment. For the other five buildings the predicted $S_{a,2}$ in general decreased with the fundamental period, e.g. for the 15-storey building the largest and lowest values of $S_{a,2}$ amounted to 4.35 g and 0.55 g, where only the largest predicted value had no effect on the MAF of collapse.

Table 3. The median $\tilde{a}_g$ based on the three different GMPEs, the standard deviation σ and the estimated upper bound $a_{g,2}$ based on 2σ and 3σ above the median, two levels of magnitude (6.5 and 7.0) and two source-to-site distances (0 and 5 km).

		M = 6.5				M = 7.0			
R_{jb} (km)	GMPE	$\tilde{a}_g$ (g)	σ	$a_{g,2}=\tilde{a}_g+2\sigma$ (g)	$a_{g,2}=\tilde{a}_g+3\sigma$ (g)	$\tilde{a}_g$ (g)	σ	$a_{g,2}=\tilde{a}_g+2\sigma$ (g)	$a_{g,2}=\tilde{a}_g+3\sigma$ (g)
0	Sabetta and Pugliese	0.68	0.17	1.51	2.25	0.97	0.17	2.15	3.20
	Akkar and Bommer	0.38	0.28	1.37	2.60	0.41	0.28	1.48	2.81
	Bindi et al.	0.32	0.34	1.52	3.31	0.45	0.34	2.14	4.66
5	Sabetta and Pugliese	0.52	0.17	1.14	1.70	0.73	0.17	1.63	2.42
	Akkar and Bommer	0.34	0.28	1.14	2.16	0.35	0.28	1.26	2.39
	Bindi et al.	0.28	0.34	1.33	2.88	0.40	0.34	1.91	4.14

Table 4. The median $\tilde{S}_a$ based on the three different GMPEs, the standard deviation σ and the estimated upper bound $S_{a,2}$ based on 2σ and 3σ above the median, two levels of magnitude (6.5 and 7.0) and two source-to-site distances (0 and 5 km) for the 4-storey building.

		M = 6.5				M = 7.0			
R_{jb} (km)	GMPE	$\tilde{S}_a$ (g)	σ	$S_{a,2}=\tilde{S}_a+2\sigma$ (g)	$S_{a,2}=\tilde{S}_a+3\sigma$ (g)	$\tilde{S}_a$ (g)	σ	$S_{a,2}=\tilde{S}_a+2\sigma$ (g)	$S_a=\tilde{S}_a+3\sigma$ (g)
0	Sabetta and Pugliese	0.70	0.26	2.29	4.16	1.26	0.26	4.14	7.51
	Akkar and Bommer	0.58	0.33	2.71	5.84	0.76	0.33	3.54	7.61
	Bindi et al.	0.58	0.35	2.97	6.72	0.91	0.35	4.64	10.5
5	Sabetta and Pugliese	0.48	0.26	1.58	2.87	0.87	0.26	2.86	5.18
	Akkar and Bommer	0.40	0.33	1.85	3.98	0.54	0.33	2.48	5.35
	Bindi et al.	0.43	0.35	2.20	4.97	0.69	0.35	3.53	8.00

The effect of the upper intensity is presented in Fig. 5 in terms of $\Delta\lambda_{C,ag2}$ and $\Delta\lambda_{C,Sa2}$ (Eqs. 3 and 5) for all six buildings. The results are presented for the marginal values of $a_{g,2}$ or $S_{a,2}$, which correspond to different GMPEs. Consideration of the maximum estimated values of the upper intensity bound did not affect the MAF of collapse since $\Delta\lambda_{C,ag2}$ and $\Delta\lambda_{C,Sa2}$ were equal to 1, whereas the minimum values of the upper bounds had a significant effect on the estimated risk, which was much more pronounced if the collapse risk assessment was based on $S_a(T_1)$ due to smaller values of the logarithmic standard deviation $\beta_{Sa,C}$ and the hazard parameter k. (see Fig. 1(b)). The largest impact of the upper integration limit was observed for the 15-storey building, whereas the smallest impact was observed for the 8-storey irregular building (Figs. 5(a) and (c)). For example, if the minimum value of the upper integration limit is taken into account and the assessment of collapse risk of the 15-storey building is based on the peak ground acceleration, then $\Delta\lambda_{C,ag2}$ amounted to 0.59 (Fig. 5(a)), which is not negligible. However, an extremely large

effect of the upper integration limit was observed in the case if the collapse risk assessment was assessed based on $S_a(T_1)$ (Fig. 5(c), $\Delta\lambda_{C,Sa2} = 0.05$). On the other hand, the impact of $a_{g,2}$ was almost negligible for the irregular 8-storey building, whereas $S_{a,2}$ substantially affected $\Delta\lambda_{C,Sa2}$, which achieved a minimum value of 0.47, indicating a possible twofold overestimation of seismic risk.

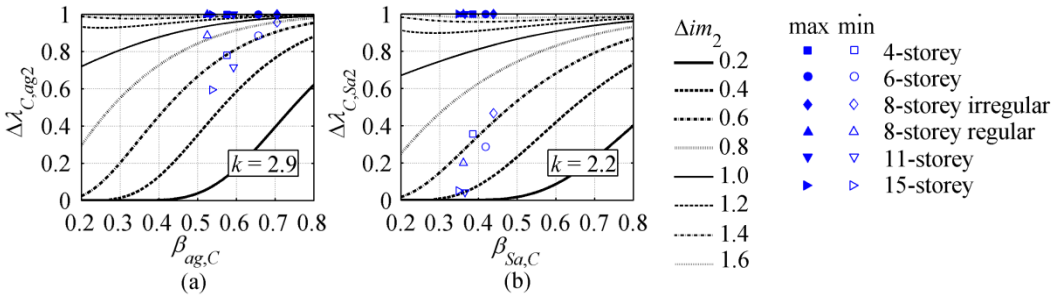

Figure 5. Point estimates of $\Delta\lambda_{C,im2}$ for the analysed buildings based on minimum and maximum im_2 for (a) a_g and $k = 2.9$ and (b) $S_a(T_1)$ and $k = 2.2$. Note that the background is based on Fig. 1(b).

Conclusions

The impact of the lower and upper integration limits on the collapse risk was investigated for six reinforced concrete frame structures based on closed-form equations, which were recently introduced. The results indicate that the mean annual frequency of collapse can be highly overestimated if intensity bounds are not considered. In general, a more significant impact of the lower integration limit can be expected if the collapse risk assessment is based on the peak ground acceleration, whereas the upper integration limit has a more pronounced effect when assessment is based on spectral acceleration at the fundamental vibration period. Additionally it was observed that the estimation of the upper intensity bounds based on GMPEs is highly uncertain. The result does not depend just on the GMPE but is also affected by the assumed upper magnitude, truncation level and source-to-site distance. Therefore reduction of uncertainties associated with the assessment of the upper bound intensity is of great importance and a challenge for seismologists.

Acknowledgments

The results presented in this paper are based on work supported by the Slovenian Research Agency. This support is gratefully acknowledged.

References

1. Pinto P, Giannini R, Franchin P. *Seismic reliability analysis of structures*. IUSS Press: Pavia, Italy, 2004.
2. Aslani H, Miranda E. Probability-based seismic response analysis. *Engineering Structures* 2005; **27**: 1151-1163.
3. Bradley BA, Dhakal RP. Error estimation of closed-form solution for annual rate of structural collapse. *Earthquake Engineering and Structural Dynamics* 2008; **37** (15): 1721-1737.

4. Vamvatsikos D. Derivation of new SAC/FEMA performance evaluation solutions with second-order hazard approximation. *Earthquake Engineering and Structural Dynamics* 2013; **42** (8): 1171-1188.

5. Cornell CA. Calculating building seismic performance reliability: a basis for multi-level design norms. *Eleventh World Conference on Earthquake Engineering*, Mexico City, Mexico, 1996.

6. Bommer JJ, Abrahamson NA, Strasser FO, Pecker A, Bard P-Y, Bungum H, Cotton F, Fäh D, Sabetta F, Scherbaum F, Studer J. The challenge of defining upper bounds on earthquake ground motions. *Seismological Research Letters* 2004; **75** (2): 82-95.

7. Strasser FO, Bommer JJ, Abrahamson NA. The need for upper bounds on seismic ground motion. *Proceedings of the 13th World Conference on Earthquake Engineering*, Vancouver, Canada, 2004.

8. Lazar N, Dolšek M. Incorporating intensity bounds for assessing the seismic safety of structures: Does it matter? *Earthquake Engineering and Structural Dynamics* 2013; DOI: 10.1002/eqe.2368.

9. Jalayer F. *Direct probabilistic seismic analysis: implementing non-linear dynamic assessments*. PhD Dissertation, Department of Civil and Environmental Engineering, Stanford University, Stanford, CA, 2003.

10. McGuire RK. *Seismic hazard and risk analysis*. Earthquake Engineering Research Institute, EERI Publication No. MNO-10, 2004.

11. CEN. *European standard EN 1998–1: 2004*. Eurocode 8: Design of structures for earthquake resistance. Part 1: General rules, seismic action and rules for buildings. European Committee for Standardization, Brussels, March, 2004.

12. EZ-FRISK Software for Earthquake Ground Motion Estimation, version 7.62. Risk Engineering, Inc., Louisville, Colorado, USA, 2012.

13. Baker JW. *Seismic hazard assessment for Ljubljana using EZ-FRISK*. Personal communication, July 2011.

14. Douglas J, Ulrich T, Negulescu C. Risk-targeted seismic design maps for mainland France. *Natural Hazards* 2012; **65** (3): 1999-2013.

15. Open System for Earthquake Engineering Simulation (OpenSees). Pacific Earthquake Engineering Research Center, 2010. Available from: http://opensees.berkeley.edu.

16. Dolšek M. Development of computing environment for the seismic performance assessment of reinforced concrete frames by using simplified nonlinear models. *Bulletin of Earthquake Engineering* 2010; **8** (6): 1309-1329.

17. Jayaram N, Lin T, Baker JW. A Computationally Efficient Ground-Motion Selection Algorithm for Matching a Target Response Spectrum Mean and Variance. *Earthquake Spectra* 2011; **27** (3): 797-815.

18. Sabetta F, Pugliese A. Estimation of Response Spectra and Simulation of Nonstationary Earthquake Ground Motions. *Bulletin of Seismological Society of America* 1996; **86** (2): 337-352.

19. Akkar S, Bommer JJ. Empirical Equations for the Prediction of PGA, PGV, and Spectral Accelerations in Europe, the Mediterranean Region, and the Middle East. *Seismological Research Letters* 2010; **81** (2): 195-206.

20. Bindi D, Pacor F, Luzi L, Puglia R, Massa M, Ameri G, Paolucci R. Ground motion prediction equations derived from the Italian strong motion database. *Bulletin of Earthquake Engineering* 2011; **9** (6): 1899-1920.

21. Lapajne J, Šket Motnikar B, Zupančič P. Probabilistic Seismic Hazard Assessment Methodology for Distributed Seismicity. *Bulletin of the Seismological Society of America* 2003; **93** (6): 2502-2515.

22. Šket Motnikar B, Lapajne J. *Revised PSHA for NPP Krško – Annex A.1.2 The influence of truncation limit in attenuation models*, PSR-NEK-2.7.2-Rev.1, 2004.

23. Beyer K, Bommer JJ. Relationships between Median Values and between Aleatory Variabilities for Different Definitions of the Horizontal Component of Motion. *Bulletin of the Seismological Society of America* 2006; **96**: 1512-1522.